Accepted Manuscript

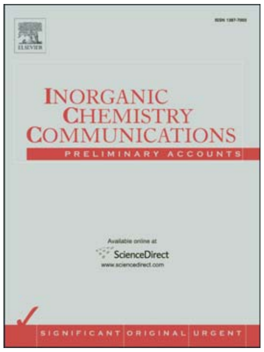

Three unique MOFs constructed by 1,4-bis(4-pyridyl)-2,3-diaza-1,3-butadiene and dicarboxylates: From rhombic tetrameric zinc(II) 2D layer to 2D + 2D → 3D polycatenated frameworks

Jie Zhou, Tong Yan, Yong-Feng Qiao, Yi-Dan Zhao, Xiao Wang, Lin Du, Ming-Jin Xie, Jian Xu, Qi-Hua Zhao

PII: S1387-7003(16)30413-0
DOI: doi:10.1016/j.inoche.2016.10.021
Reference: INOCHE 6458

To appear in: *Inorganic Chemistry Communications*

Received date: 20 July 2016
Revised date: 1 October 2016
Accepted date: 7 October 2016

Please cite this article as: Jie Zhou, Tong Yan, Yong-Feng Qiao, Yi-Dan Zhao, Xiao Wang, Lin Du, Ming-Jin Xie, Jian Xu, Qi-Hua Zhao, Three unique MOFs constructed by 1,4-bis(4-pyridyl)-2,3-diaza-1,3-butadiene and dicarboxylates: From rhombic tetrameric zinc(II) 2D layer to 2D + 2D → 3D polycatenated frameworks, *Inorganic Chemistry Communications* (2016), doi:10.1016/j.inoche.2016.10.021

Three unique MOFs constructed by 1,4-bis(4-pyridyl)-2,3-diaza-1,3-butadiene and dicarboxylates: from rhombic tetrameric Zinc(II) 2D layer to 2D + 2D → 3D polycatenated frameworks

Jie Zhou [a], Tong Yan [a], Yong-Feng Qiao [a], Yi-Dan Zhao [a], Xiao Wang [a], Lin Du [a], Ming-Jin Xie [a], Jian Xu [a], Qi-Hua Zhao [a]*

[a] *Key Laboratory of Medicinal Chemistry for Natural Resource Education Ministry, School of Chemical Science and Technology, Yunnan University, Kunming, 650091, P. R. China*

* Corresponding Author. Tel: +86 871 5032929; fax: +86 871 5032929. E-Mail: qhzhao@ynu.edu.cn

Abstract: Three metal–organic networks, namely, $[Zn_2(Hnip)(4\text{-bpdb})(nip)_2(\mu_3\text{-OH})]$ (**1**), $\{[Zn(tbip)(4\text{-bpdb})_{1.5}]\cdot CH_3OH\}_n$ (**2**), and $\{[Ni(1,3\text{-bdc})(4\text{-bpdb})]\cdot 2H_2O\}_n$ (**3**) (4-bpdb = 1,4-bis(4-pyridyl)-2,3-diaza-1,3-butadiene, H_2nip = 5-nitroisophthalic acid, H_2tbip = 5-*tert*-butylisophthalic acid, and 1,3-H_2bdc = 1,3-benzenedicarboxylic acid) are synthesized under hydrothermal conditions. The structure of **1** is built around uncommon rhombic $\{Zn_4\}$ clusters with double T_d and double O_h Zn(II) geometries, which extend into a 2D network by the rigid deprotonated H_2nip and 4-bpdb bridges. Meanwhile, **2** presents a novel 2D → 3D parallel polycatenated framework assembled from 2D bilayers with cuboids as the fundamental building units. Compound **3** features an interesting 2D → 3D inclined polycatenated network based on 4^4-**sql** subunits. Moreover, the thermal stabilities, photoluminescence, and magnetic properties of the compounds are also discussed.

Keywords: Bis-pyridyl ligand; Coordination polymer; Crystal structure; Magnetic property; Polycatenated framework

The synthesis and characterization of novel coordination polymers (CPs) remain under intensive investigation not only assess their unique architectures but also to understand the fundamental scientific laws underlying the coordination behavior of molecular systems [1]. Among the new and numerous coordinated CPs, cluster-based frameworks [2] and polycatenated networks [3] have attracted particular attention because of their interesting features and aesthetic structures. Most of the cluster-based CPs are obtained using oxo-centered metal clusters, whereas the incorporation of μ-hydroxyl group is likely to induces the aggregation of metal cores to form clusters. Noteably, most of the reported cluster-based CPs possess 3D structures, whereas only a few CPs possess 2D structures [4]. Meanwhile, polycatenations comprise a relatively rare branch of entangled systems and have a higher dimensionality than that of component motifs. Some fascinating polycatenation associations have been documented. Among these polycatenations, the higher-dimensional motifs, i.e., 2D → 3D polycatenations, are relatively less common [5].

Recently, mixed-ligand CPs generated from multicarboxylate acids and N-containing linkers have attracted intensive interest because of their ability to incorporate the virtues of different functional groups and to easily obtain controlled architecture by changing one of the ligands [6]. Aromatic dicarboxylate ligands [7] are among the most commonly employed linkers in this field, providing the structural rigidity and charge balance necessary to avoid the inclusion of unligated anionic species. The geometric orientation and binding mode of the carboxylate groups, the coordination preferences for specific metal ions, and the self-assembly of metal carboxylate cluster subunits act synergistically to produce diverse structural topologies. Angular dicarboxylates, such as 1,3-benzenedicarboxylic acid (1,3-H_2bdc) and its derivative, have been used as notable organic spacers for the construction of CPs in conjunction with various N-donor ligands because of their diverse coordination capabilities and topological–directional preferences [8]. With conformational freedom, 1,4-bis(4-pyridyl)-2,3-diaza-1,3-butadiene (4-bpdb) has been justified as an efficient organic building unit for the construction of coordination architectures [9]. However, the use of 4-bpdb in combination with multicarboxylate ligands is still limited and has attracted considerable attention only recently [10].

Given the aforementioned consideration and our previous work [11], three novel cluster-based and polycatenated CPs based on 4-bpdb and angular dicarboxylates ligands, namely $[Zn_2(Hnip)(4\text{-bpdb})(nip)_2(\mu_3\text{-OH})]$ (**1**), $\{[Zn(tbip)(4\text{-bpdb})_{1.5}]\cdot CH_3OH\}_n$ (**2**), and $\{[Ni(1,3\text{-bdc})(4\text{-bpdb})]\cdot 2H_2O\}_n$ (**3**) (H_2nip = 5-nitroisophthalic acid, H_2tbip = 5-*tert*-butylisophthalic acid, and 1,3-H_2bdc = 1,3-benzenedicarboxylic acid), were obtained. Their syntheses, crystal structures, topologies, thermal stabilities, photoluminescence, and magnetic properties are reported in this study.

Complexes **1**–**3** were isolated under similar hydrothermal conditions, but by using different molar ratios of metal/4-bpdb/dicarboxylic acid. The crystallographic data and detailed procedure of the synthesis of the complexes are given in the ESI. The selected bond lengths and angles are listed in Table S1. The topological analysis and some diagrams were produced using the TOPOS program [12].

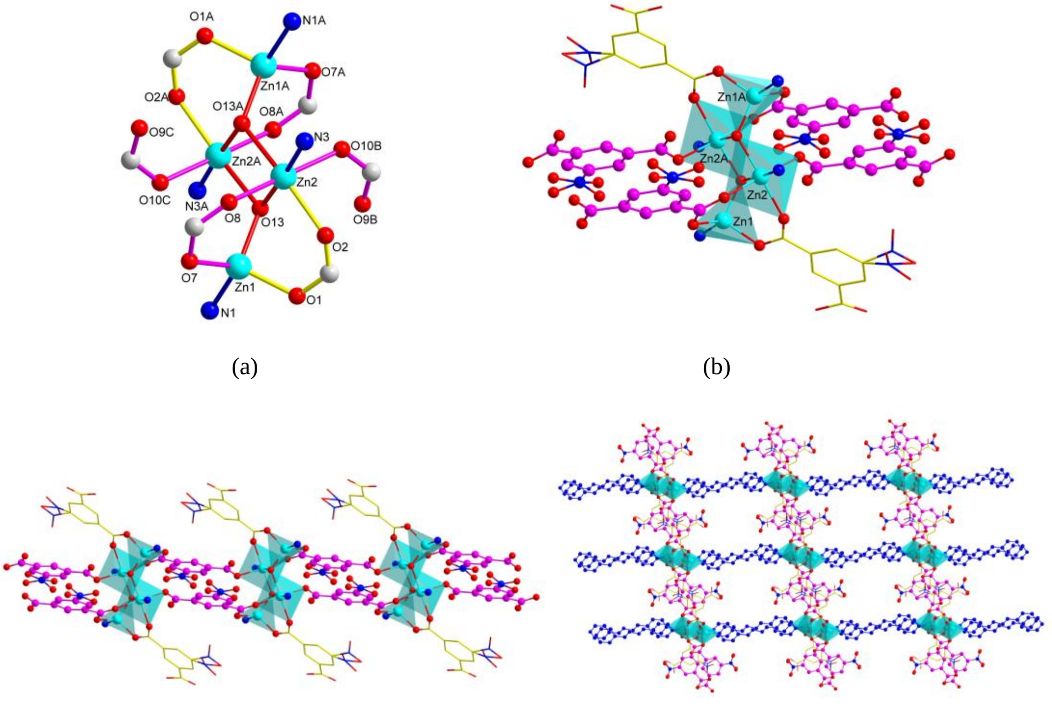

(a) (b)

(c) (d)

Fig. 1. (a) The Zn_4-cluster and the coordination around two tetrahedral and two octahedral zinc atoms of **1** {the Zn(II) atoms are highlighted with polyhedral, symmetry codes: (A) $-x + 1, -y + 1, -z$; (B) $x + 1, y, z$; (C) $-x, -y +$

1, −*z*}. (b) The 1D ribbon of [$Zn_4(\mu_3\text{-}OH)_2(Hnip)_2(nip)_4$]. (c) The 2D layer of compound **1** (the 4-bpdb spacers are highlighted with blue color).

Complex **1** has a unique 2D double-layered framework containing rhombic tetrameric Zn(II) of mixed T_d and O_h geometries. Single-crystal X-ray diffraction shows that **1** crystallizes in the triclinic system with the $P\bar{1}$ space group. The asymmetric unit of **1** contains two Zn(II) atoms, one Hnip^{2-} anions, two nip^{2--} anions, one 4-bpdb ligand, and one hydroxyl group. Zn1 has a distorted {ZnNO3} tetrahedral geometry ($\tau = 0.093$) [13] surrounded by one nitrogen atom of 4-bpdb, one carboxylate oxygen atom from the fully deprotonated nip^{2-} molecule, one carboxylate oxygen atom from an incompletely deprotonated Hnip^{-}, and one hydroxyl oxygen atom. Meanwhile, Zn2 is six-coordinated, showing distorted octahedral configurations, which are defined by one nitrogen atom of 4-bpdb, two carboxylate oxygen atoms from two different nip^{2-} groups, one carboxylate oxygen atom from Hnip^{-} group, and two hydroxyl oxygen atoms {Fig. 1(a)}. In **1**, two symmetrically related μ_3-OH^{-} groups (symmetry code: $-x + 1$, $-y + 1$, $-z$) connect four Zn(II) atoms to form a rhombic [$Zn_4(\mu_3\text{-}OH)_2$]$^{8+}$ cluster subunit. Such cluster is held together by six carboxylate groups, thereby constituting the tetranuclear [$Zn_4(\mu_3\text{-}OH)_2(COO)_6$] cluster. Within the cluster, four Zn(II) ions are totally coplanar, and the different Zn···Zn clusters measure 3.139 (Zn1···Zn2), 3.599 (Zn1···Zn2A), and 3.217 Å (Zn2···Zn2A) {Fig. 1(b)}.

Two kinds of deprotonated H_2nip anions exist, (μ_2-η^1:η^1)-Hnip^{-} and (η^1)(μ_2-η^1:η^1)-nip^{2-} [14]. Two nip^{2-} ligands bridge two neighboring tetramers with carboxylate groups in a monodentate and mono/bidentate (*syn*–*syn*) bridging mode, whereas Hnip^{-} terminal ligands act as side arms, generating a neutral 1D [$Zn_4(\mu_3\text{-}OH)_2(Hnip)_2(nip)_4$] ribbon along the *a* axis {Fig. 1(c)}. The Zn_4···Zn_4 distance separated by the nip linker is 10.915 Å. The ribbons are parallel to one another and are further interlinked into 2D 4,4′-layer by 4-bpdb ligands with a ribbon–ribbon distance of approximately 18.363 Å {Fig. 1(d)}.

Further investigation of the crystal packing reveals that these parallel 4,4′-nets are extended through a staggered disposition, and terminal Hnip^{-} ligands are embedded in the square grids of adjacent layers. As a consequence, such arrays are interdigitated with the presence of interlayer strong O–H···O contacts where uncoordinated carboxyl oxygen atoms (O3) interact with uncoordinated Hnip^{-} carboxyl oxygen atoms (O9) of adjacent layers with bond lengths of 2.588 Å (O3···O9) (Figs. S1 and S2).

Remarkably, cluster-based CPs with 2D frameworks are few. The complex [$Zn_4(\mu_3\text{-}OH)_2$(5-NIP)$_4$(TBPE)$_2$] (where 5-NIP = 5-nitro isophthalic acid and TBPE = trans-4,4′-bipyridylethylene), possesses a 2D structure similar to **1**, as reported recently. However, [$Zn_4(\mu_3\text{-}OH)_2$(5-NIP)$_4$(TBPE)$_2$] was incorrectly described as a 3D complex [15].

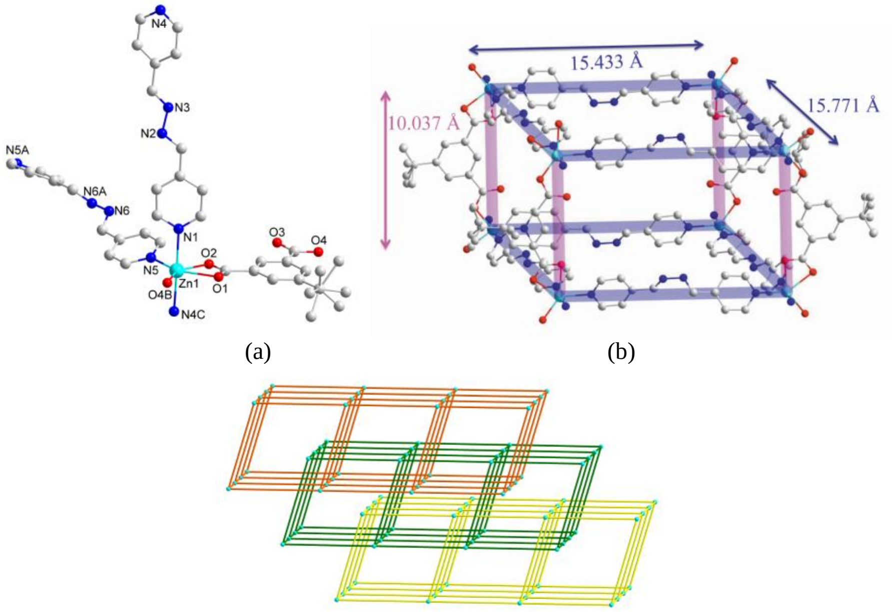

(a) (b)

(c)

Fig. 2 (a) Coordination environment of Zn(II) atoms of **2** (Symmetry codes: (A) $-x + 1$, y, $-z + 1/2$; (B) x, $y + 1$, z; (C) $x + 1/2$, $-y + 1/2$, $z + 1/2$). (b) The cuboidal box of **2**. (c) Schematic illustration of the parallel polycatenation in **2**.

Substituted groups in polycarboxylates may influence the resulting structures of the final products. Products with different topological structures may be obtained by rational design and tuning of the substituted groups of the polycarboxylate ligands [16]. Thus, another substituted group, $–C(CH_3)_3$, was considered because of its large steric hindrance and H_2tbip was involved in the construction of compound **2**. Single-crystal X-ray diffraction reveals that **2** shows a 2D + 2D → 3D parallel polycatenated framework, which contains 2D bilayers with cuboids as the fundamental building units. The compound crystallizes in the monoclinic space group C2/c, the asymmetric unit of **2** contains one Zn(II) atom, one and a half 4-bpdb ligands, one tbip$^{2–}$ anion, and one uncoordinated methanol molecule. Each Zn(II) center has a slightly distorted {ZnN3O3} octahedral coordination sphere and coordinated by two nitrogen atoms from two 4-bpdb ligands occupying the axial positions, whereas the equatorial positions are defined by two oxygen atoms from the chelating carboxylic group of a tbip$^{2–}$ ligand, one oxygen atom from a monodentate carboxylic group of a second but symmetry related tbip$^{2–}$ ligand, and one nitrogen atom of 4-bpdb ligand (Fig. 2 (a)).

The Zn(II) centers are first linked by the 4-bpdb linkers to form 1D double-chain ladders consisting of cationic $[Zn(4\text{-bpdb})_{1.5}]^{2+}$ squares with Zn···Zn distances of 15.771 and 15.433 Å (Fig. S3).Then, the square units of the ladders are joined by tbip$^{2–}$ bridges with the carboxylate groups in the monodentate (η^1) and chelating (η^2) modes, resulting in a 2D bilayer motif with cuboidal box consisting of eight Zn(II) atoms at the corners {Fig. 2(b)}. Thus, **2** is a five-connected uninodal net with a point symbol of $(4^8{\cdot}6^2)$ [17].

Large regular 1D channels are evident in **2** (Figs. S4 and S5). The large channels result in an interesting and peculiar structural feature of **2**, that is, each layer motif polycatenated with two adjacent (the upper and the lower) and parallel identical motifs (DOC = 2) [18] result in a 2D + 2D → 3D polycatenated framework {Fig. 2(c)}. In addition, the effective free volume (7.01%, 440.9 Å^3 out of the 6,245.3 Å^3 unit cell volume) [19] remains even after interpenetration and becomes occupied by uncoordinated methanol molecules (Fig. S6).

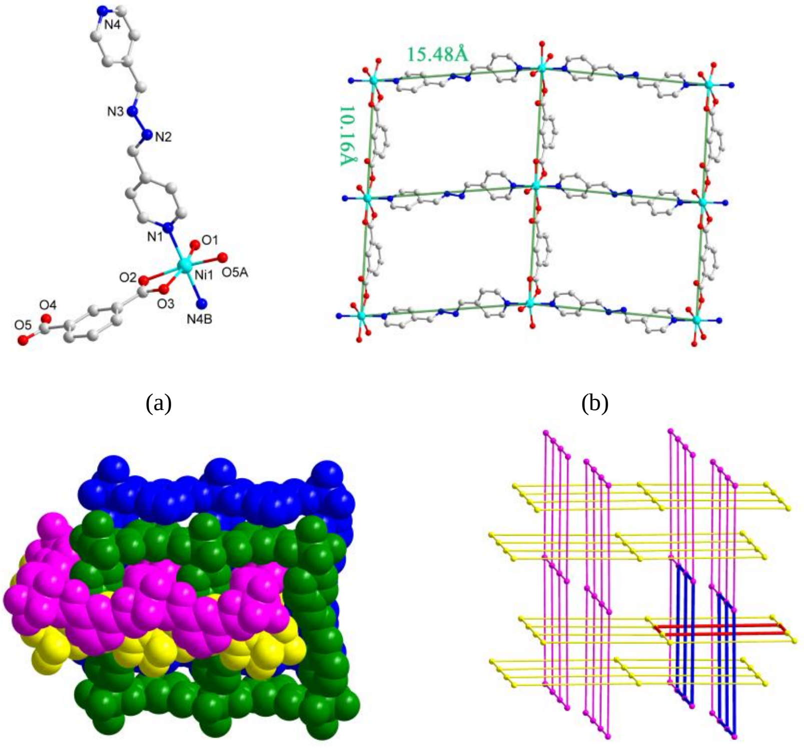

(a) (b)

(c) (d)

Fig. 3. (a) Coordination environment of the Ni(II) atom (symmetry codes: (A) $x, y, -z + 1$; (B) $x + 1/2, y - 1/2, -z$). (b) A view of the 2D 4^4-**sql** layer in **3**. (c) Catenation through Hopf links in the parallel–parallel (p–p) arrangement in **3**. (d) Schematic of the inclined polycatenation in **3**.

Single-crystal X-ray analysis reveals that compound **3** crystallizes in the centrosymmetric tetragonal $P4_2/n$ space group. The asymmetric unit contains one Ni(II) atom, one 1,3-bdc$^{2–}$, one

4-bpdb ligand, one coordinated water molecule, and two lattice water molecules squeezed by PLATON software [20]. Ni1 is in a slightly distorted [NiN2O4] octahedral coordination sphere and coordinated by three carboxylate oxygen atoms from two 1,3-bdc^{2-} anions and one water oxygen molecule at the equatorial plane, and the axial position is occupied by two nitrogen atoms from two 4-bpdb molecules {Fig. 3(a)}. The Ni–O and Ni–N bond lengths are all within the normal ranges.

Further expansion of the structure occurs through the monodentate/bridging and chelating 1,3-bdc^{2-} anions, and 4-bpdb ligands create a (4,4) rhomboid grid CP layer {Fig. 3(b)}. Within each layer, the rhomboid windows have dimensions of 10.16 Å× 15.48 Å with angles of 94.61° and 85.39° (defined by Ni···Ni distances and Ni···Ni···Ni angles).

Packing of the layers generates two sets of layers oriented toward different directions. The large size of the grids in the two individual (4,4) nets allows interpenetration. Further insight into one window of a layer reveals that each window is catenated with four other windows from two different layers in the other set through Hopf links in a p–p arrangement with the density of catenation = (4/4) {Figs. 3(c) and 3(d)}. Thus, the entanglement of these two sets of 2D 4^4-**sql** layers results in a 2D + 2D → 3D-inclined polycatenated framework [5, 21].

As shown previously, the simultaneous use of the conformational freedom 4-bpdb ligand and polycarboxylic acids produce various CPs of novel architectures. Generally, the diverse structures are mainly attributed to the different geometric requirements of metal centers and various coordination modes and conformations of the two kinds of ligands. For example, considering **1** and **2**, the two kinds of dicarboxylate (Hnip^{-} and nip^{2-} in **1** and tbip^{2-} in **2**) with different substituents lead to different coordination geometries of the carboxylates and result in totally different architectures. In addition, bpdb ligands with conformational freedom are important in the assembly of the terminal structures of the complexes. Regarding **2** and **3**, although carboxylic acid ligands in the two CPs are different (H_2tbip in **2** and 1,3-H_2bdc in **3**), the coordination geometry of the metal ions is similar. The difference in the structures is mainly attributed to the rotational bpdb ligands. Notably, the two pyridyl rings of 4-bpdb are not coplanar and form a dihedral angle of 32.5° in **2** and 136.5° in **3** through the rotation of the diaza group R–C=N–N=C–R (Scheme S1).

The thermal behavior of Complexes **1**–**3** was investigated under nitrogen atmosphere a heating rate of 10 °C min^{-1} by TGA to characterize their thermal stabilities (Fig. S7). Complex **1** remained stable up to approximately 340 °C; then, the framework collapsed. The TG curve for **2** shows a gradual weight loss between 78 °C and 115 °C, which can be ascribed to the removal of free methanol molecules (observed, 4.92%; calculated, 5.19%). The removal of organic ligands starts at 350 °C. The remaining weight corresponds to the formation of ZnO (observed, 13.01%; calculated, 13.49%). For **3**, the initial weight loss between 40 °C and 210 °C is attributed to the release of lattice water and one coordinated water molecule (observed, 11.79%; calculated, 11.10%). The decomposition of the anhydrous composition occurs at 325 °C to 420 °C. The 17.56% residue at 800 °C is assigned to nickel oxide residue (calculated, 15.33%).

The solid-state photoluminescence properties of d^{10} metal Complexes **1** and **2** as well as 4-bpdb ligand have been investigated in their solid state at room temperature (Fig. S8). 4-bpdb displays a broad band with a maximum peak at 530 nm and two shoulder peaks at approximately 475 and 496 nm (λ_{ex} = 375 nm). Presumably, the peaks originate from the $\pi^* \rightarrow \pi$ transition. To the best of our knowledge, the emission of dicarboxylate belongs to

$\pi^* \rightarrow n$ transitions, which are weaker than that of the $\pi^* \rightarrow \pi$ transition of the bpdb. Thus, the dicarboxylate has almost no contribution to the fluorescent emission of the as-synthesized complexes. Complex **1** displays photoluminescence with maximum emission at 470 nm (λ_{ex} = 305 nm). Meanwhile, excitation at 375 nm leads to three intense fluorescent emission bands with the peak at approximately 473/484/494 nm for Complex **2**. The emissions for **1** and **2** can be tentatively assigned to the $\pi^* \rightarrow \pi$ intraligand fluorescence [10a, 22] because of their close resemblance to the emission band.

Variable-temperature magnetic susceptibility measurements were performed on powdered crystalline samples of Complex **3** in a 1,000 Oe field in the 2 K to 300 K range. The obtained data for Complex **3** are shown as the χ_M^{-1} (inset), χ_M, and $\chi_M T$ versus T plots in Fig. 4. From the data of the χ_M^{-1} versus T plot, the magnetic behavior of the complex follows the Curie–Weiss law, $\chi_M = C/(T - \theta)$, in the entire range of temperature with a Curie constant (C) value of 1.292 cm^3 K mol^{-1} and a Weiss temperature θ of −2.532 K. The perfect linear relationship in the plot reveals a system with weak antiferromagnetic interactions. From the $\chi_M T$ versus T plot of **3**, the $\chi_M T$ value is 1.29 cm^3 mol^{-1} K at room temperature. Overall, the $\chi_M T$ value decreases with the decrease in temperature, and the value slowly decreases from approximately 300 K to 20 K. However, a dramatic decrease in the value below 20 K to 0.54 cm^3 mol^{-1} K at 2 K was observed. The data were analyzed, assuming the presence of isotropic Heisenberg pairwise interactions between nickel ions in a linear chain and using the following equations:

$$\chi' = \frac{Ng^2\beta^2 S(S+1)}{3kT}\frac{(1-u)}{(1+u)}$$

$$u = \coth\left[\frac{2JS(S+1)}{kT}\right] - \frac{kT}{2JS(S+1)}$$

$$\chi_M = \chi' / [1 - (zj'\chi' / Ng^2\beta^2)]$$

The best fit to the experimental data gives g = 2.25, J = −0.8176 cm^{-1}, zj' = 0.0551 cm^{-1}, and $R = 6.1 \times 10^{-5}$ (R is defined as $\Sigma[(\chi_M)_{obs} - (\chi_M)_{calcd}]^2/\Sigma(\chi_M)_{obs}{}^2$). The fitting results confirm that weak antiferromagnetic coupling exists between Ni(II) ions. The fitting result is comparable with those reported for Ni(II) CPs [23].

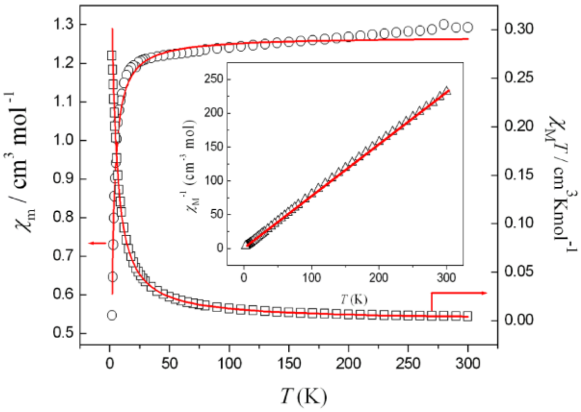

Fig. 4. Temperature dependence of the $\chi_M T$ (Δ) and χ_M (□) products at 1,000 Oe for **3**. The solid lines correspond to the theoretical fits.

In summary, we successfully synthesized and characterized three unique coordination polymers based on conformational freedom of 4-bpdb ligand and angular dicarboxylate ligands.The complexes exhibit a 2D network with rhombic {Zn_4} clusters, a parallel and a inclined 2D → 3D polycatenated framework, respectively. In addition, the photoluminescent properties of **1** and **2** and the magnetic properties of **3** were investigated.

Acknowledgement

This work was supported by NSFC (Projects 21371151, 21461029 and 21561033) and NSF of Yunnan Province (Project 2016FB023).

Appendix A. Supplementary data

CCDC reference numbers 1442218 (**1**), 1442219 (**2**), and 1442220 (**3**) contain the supplementary crystallographic data for this paper. These data can be obtained free of charge via www.ccdc.can.ac.uk/data_request/cif (or from the Cambridge Crystallographic Centre, 12 Union Road, Cambridge CB21EZ, UK; Fax: (+44) 1223-336033; or deposit@ccdc.cam.ac.uk). Crystallographic data, selected bond lengths and angles, additional structural figures, thermal stabilities, photoluminescence, IR, PXRD patterns for **1**–**3**, these data can be found in the supporting file. Supplementary data associated with this article can be found in the online version, at http .

References

[1] (a) H. Furukawa, K. E. Cordova, M. O' Keeffe, O. M. Yaghi, Science 341 (2013) 1230444. (b) M. Li, D. Li, M. O'Keeffe, O. M. Yaghi, Chem. Rev. 114 (2013) 1343-1370. (c) R.-J. Li, M. Li, X.-P. Zhou, D. Li, M. O'Keeffe, Chem. Commun. 50 (2014) 4047-4049. (d) G. Wang, T. Song, Y. Fan, J. Xu, M. Wang, H. Zhang, L. Wang, L. Huang, L. Wang, Inorg. Chem. Commun.13, (2010) 502-505.

[2] (a) D.-M. Chen, X.-Z. Ma, X.-J. Zhang, N. Xu, P. Cheng, Inorg. Chem. 54 (2015) 2976-2982. (b) U. Schubert, Chem. Soc. Rev. 40 (2011) 575-582. (c) Z. Y. Liu, E. C. Yang, X. J. Zhao, Inorg. Chem. Commun. 70, (2016) 197-200.

[3] (a) C. Zhang, C. Chen, S. Liu, N. Zhang, Inorg. Chem. Commun. 20 (2012) 18-22. (b) A. D. Sample, R. L. LaDuca, Inorg. Chim. Acta 443 (2016) 198-206. (c) W. Xia, P. Tang, X.-Q. Wu, J. Cui, D.-S. Li, W.-W. Dong, J. Y. Lu, Inorg. Chem. Commun. 51 (2015) 17-20. (d) H. Xu, G.-L. Bao, C.-H. Zhu, J.-Y. Sun, R.-Y. Huang, Inorg. Chem. Commun. 69 (2016) 75-78.

[4] (a) Y.-Y. Zhang, H. Zhao, E.-C. Yang, Z.-Y. Liu, Q. Shang, X.-J. Zhao, Dalton Trans. 44 (2015) 5826-5836. (b) J. Tao, M.-L. Tong, J.-X. Shi, X.-M. Chen, S. W. Ng, Chem. Commun. (2000) 2043-2044. (c) H.-H. Zou, X.-H. Yin, X.-J. Sun, Y.-L. Zhou, S. Hu, M.-H. Zeng, Inorg. Chem. Commun. 13 (2010) 42-45.

[5] (a) Q. Yang, Y. Chen, X. Li, Y.-C. Xu, J. Li, D.-R. Xiao, Inorg. Chim. Acta 444 (2016) 56-62. (b) B. Xu, Z. Lin, L. Han, R. Cao, CrystEngComm 13 (2011) 440-443. (c) D. Sun, Z.-H. Yan, Y.-K. Deng, S. Yuan, L. Wang, D.-F. Sun, CrystEngComm 14 (2012) 7856-7860. (d) X-C. Wang, Q. Yang, J. Li, H-L. Xu, H. Yuan, D-R. Xiao, Inorg. Chim. Acta 2016 doi: http://dx.doi.org/10.1016/j.ica.2016.07.018

[6] (a) M. Du, C.-P. Li, C.-S. Liu, S.-M. Fang, Coord. Chem. Rev. 257 (2013) 1282-1305. (b) Z. Yin, Y.-L. Zhou, M.-H. Zeng, M. Kurmoo, Dalton Trans. 44 (2015) 5258-5275. (c) X. Feng, J. L. Chen, R. F. Bai, L. Y. Wang, J. T. Wei, X. X. Chen, Inorg. Chem. Commun. 66 (2016) 41-46. (d) Y.-J. Ping, R.-Y. Yan, G.-C. Zhao, L. Qin, H.-G. Zheng, Inorg. Chem. Commun. 61 (2015) 136-139.

[7] (a) J. J. Perry Iv, J. A. Perman, M. J. Zaworotko, Chem. Soc. Rev. 38 (2009) 1400-1417. (b) L. Zhang, Z.-J. Li, Q.-P. Lin, Y.-Y. Qin, J. Zhang, P.-X. Yin, J.-K. Cheng, Y.-G. Yao, Inorg. Chem. 48 (2009) 6517-6525. (c) B. Fernández, J. M. Seco, J. Cepeda, A. J. Calahorro, A. Rodríguez-Diéguez, CrystEngComm 17 (2015) 7636-7645. (d) J. M. Hu, K. Van Hecke, B. Yu, G. H. Cui, Inorg. Chem. Commun. 61, (2015) 217-220.

[8] (a) Y. Rachuri, B. Parmar, K. K. Bisht, E. Suresh, Inorg. Chem. Front. 2(2015) 228-236. (b) L. Gao, B. Zhao, G. Li, Z. Shi, S. Feng,Inorg. Chem. Commun. 6, (2003) 1249-1251.

[9] (a) C.-C. Wang, W.-Z. Lin, W.-T. Huang, M.-J. Ko, G.-H. Lee, M.-L. Ho, C.-W. Lin, C.-W. Shih, P.-T. Chou, Chem. Commun. (2008) 1299-1301. (b) M. Ghazzali, V. Langer, K. Larsson, L. Öhrström, CrystEngComm 13 (2011) 5813-5817. (c) L. Hashemi, A. Morsali, CrystEngComm 16 (2014) 4955-4958. (d) M. Anindita, C. Rajesh,K. P. Goutam, Inorg. Chem. Commun.12, (2009) 1227-1230.

[10] (a) S. Su, C. Qin, Z. Guo, H. Guo, S. Song, R. Deng, F. Cao, S. Wang, G. Li, H. Zhang, CrystEngComm 13 (2011) 2935-2941. (b) D. K. Maity, B. Bhattacharya, A. Halder, A. Das, D. Ghoshal, Polyhedron 102 (2015) 634-642. (c) D. Singh, C. M. Nagaraja, Cryst. Growth Des. 15 (2015) 3356-3365. (d) B. Bhattacharya, D. K. Maity, R. Mondal, E. Colacio, D. Ghoshal, Cryst. Growth Des. 15 (2015) 4427-4437.

[11] (a) J. Zhou, L. Du, Y.-F. Qiao, Y. Hu, B. Li, L. Li, X.-Y. Wang, J. Yang, M.-J. Xie, Q.-H. Zhao, Cryst. Growth Des. 14 (2014) 1175-1183. (b) Q. H. Zhao, Y. Q. Liu, R. B. Fang, Inorg. Chem. Commun. 9 (2006) 699-702. (c) J. Zhou, S.-F. Dong, Y.-F. Qiao, L. Du, T. Yan, M.-J. Xie, Q.-H. Zhao, Chin. J. Inorg. Chem. 31 (2015) 2095-2102.

[12] Net topology was calculated by the TOPOS program. See: V. A. Blatov, TOPOS, A Multipurpose Crystallochemical Analysis with the Package, Samara State University, Russia, 2004.

[13] A. W. Addison, T. N. Rao, J. Reedijk, J. van Rijn, G. C. Verschoor, J. Chem. Soc., Dalton Trans. (1984) 1349-1356.

[14] (a) Bu, G. B. Deacon, M. Hilder, P. C. Junk, U. H. Kynast, W. W. Lee, D. R. Turner, CrystEngComm 9 (2007) 394-411. (b) G. B. Deacon, S. Hein, P. C. Junk, T. Jüstel, W. Lee, D. R. Turner, CrystEngComm 9 (2007) 1110-1123.

[15] M. K. Bhunia, S. K. Das, M. M. Seikh, K. V. Domasevitch, A. Bhaumik, Polyhedron 30 (2011) 2218-2226.

[16] (a) S. Das, I. Gupta, Inorg. Chem. Commun. 60 (2015) 54-60. (b) L.-L. Liu, C.-X. Yu, F.-J. Ma, Y.-R. Li, J.-J. Han, L. Lin, L.-F. Ma, Dalton Trans. 44 (2015) 1636-1645. (c) N. Urdaneta, V. R. Landaeta, R. E. Rodríguez-Lugo, C. Díaz, G. Santiso-Quinones, J. Quiroga, B. Insuasty, Inorg. Chem. Commun. 55 (2015) 43-47.

[17] (a) Z.-Y. Fu, X.-T. Wu, J.-C. Dai, L.-M. Wu, C.-P. Cui, S.-M. Hu, Chem. Commun. (2001) 1856-1857. (b) X. L. Wang, C. Qin, E. B. Wang, Y. G. Li, Z. M. Su, L. Xu, L. Carlucci, Angew. Chem. Int. Ed. 44 (2005) 5824-5827. (c) B. Liu, D. S. Li, L. Hou, G. P. Yang, Y. Y. Wang, Q. Z. Shi, Dalton Trans. 42 (2013) 9822-9825. (d) B. Xu, J. Li, N. Kong, C. Li, Inorg. Chem. Commun. 47 (2014) 119-122.

[18] (a) L. Carlucci, G. Ciani, D. M. Proserpio, Coord. Chem. Rev. 246 (2003) 247-289. (b) A. Baburin, V. A. Blatov, L. Carlucci, G. Ciani, D. M. Proserpio, CrystEngComm 10 (2008) 1822-1838. (c) L. Carlucci, G. Ciani, D. M. Proserpio, T. G. Mitina, V. A. Blatov, Chem. Rev. 114 (2014) 7557-7580.

[19] A. L. Spek, J. Appl. Crystallogr. 36 (2003) 7–13.

[20] Platon Program: A. L. Spek, Acta Crystallogr. Sect. A: Found. Crystallogr. 46 (1990) 194.

[21] (a) X.-T. Zhang, D. Sun, B. Li, L.-M. Fan, B. Li, P.-H. Wei, Cryst. Growth Des. 12 (2012) 3845-3848. (b) X.-J. Ke, D.-S. Li, J. Zhao, L. Bai, J.-J. Yang, Y.-P. Duan, Inorg. Chem. Commun. 21 (2012) 129-132. (c) P. Thuéry, J. Harrowfield, Inorg. Chem. 54 (2015) 8093-8102.

[22] (a) C.-C. Wang, G.-B. Sheu, S.-Y. Ke, C.-Y. Shin, Y.-J. Cheng, Y.-T. Chen, C.-H. Cho, M.-L. Ho, W.-T. Chen, R.-H. Liao, CrystEngComm 17 (2015) 1264-1272. (b) Y.-H. Tan, J.-B. Xiong, J.-X. Gao, Q. Xu, C.-W. Fu, Y.-Z. Tang, S.-P. Yang, H.-R. Wen, Q. Shu, RSC Adv. 5 (2015) 30216-30221. (c) T. Yu, V. K.-M. Au, D. P.-K. Tsang, M.-Y. Chan, V. W.-W. Yam, Dalton Trans. 44 (2015) 18983-18992.

[23] (a) X.-Q. Wu, M.-L. Han, G.-W. Xu, B. Liu, D.-S. Li, J. Zhang, Inorg. Chem. Commun. 58 (2015) 60-63. (b) H. Zhou, X. H. Chen, W. W. Sun, Y. Mei, Z. Q. Pan, RSC Adv. 4 (2015) 5080-5084. (c) T.-F. Liu, Z.-X. Wang, Inorg. Chem. Commun. 30 (2013) 84-87.

Three unique MOFs constructed by 1,4-bis(4-pyridyl)-2,3-diaza-1,3-butadiene and dicarboxylates: from rhombic tetrameric Zinc(II) 2D layer to 2D + 2D → 3D polycatenated frameworks

Jie Zhou [a], Tong Yan [a], Yong-Feng Qiao [a], Yi-Dan Zhao [a], Xiao Wang [a], Lin Du [a], Ming-Jin Xie [a], Jian Xu [a],
Qi-Hua Zhao [a]*

[a] *Key Laboratory of Medicinal Chemistry for Natural Resource Education Ministry, School of Chemical Science and Technology, Yunnan University, Kunming, 650091, P. R. China*

* Corresponding Author. Tel: +86 871 5032929; fax: +86 871 5032929. E-Mail: qhzhao@ynu.edu.cn

Graphical abstract-Pictogram

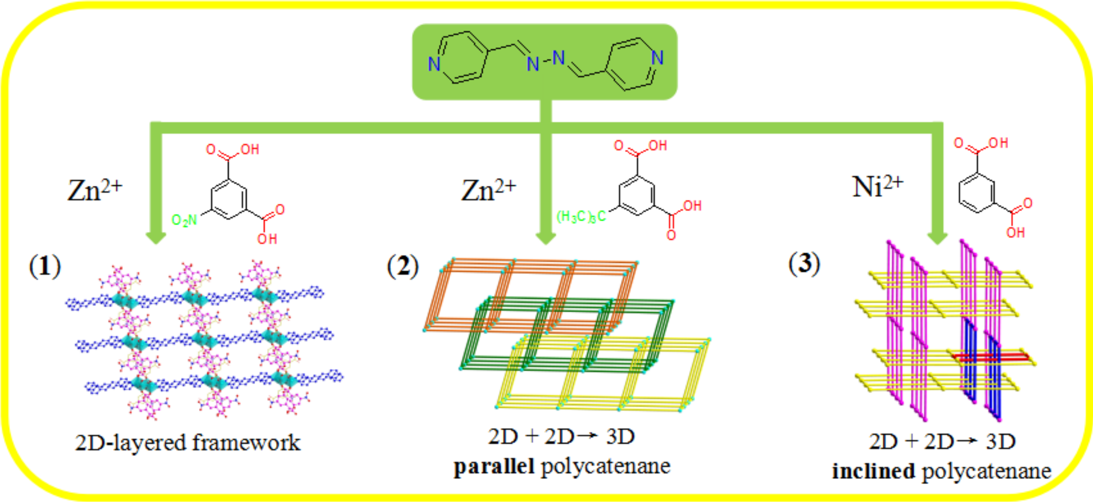

Three unique MOFs constructed by 1,4-bis(4-pyridyl)-2,3-diaza-1,3-butadiene and dicarboxylates: from rhombic tetrameric Zinc(II) 2D layer to 2D + 2D → 3D polycatenated frameworks

Jie Zhou [a], Tong Yan [a], Yong-Feng Qiao [a], Yi-Dan Zhao [a], Xiao Wang [a], Lin Du [a], Ming-Jin Xie [a], Jian Xu [a], Qi-Hua Zhao [a]*

[a] *Key Laboratory of Medicinal Chemistry for Natural Resource Education Ministry, School of Chemical Science and Technology, Yunnan University, Kunming, 650091, P. R. China*

* Corresponding Author. Tel: +86 871 5032929; fax: +86 871 5032929. E-Mail: qhzhao@ynu.edu.cn

Graphical abstract-Synopsis

Three coordination polymers are reported: compound **1** exhibit a 2D network with rhombic $\{Zn_4\}$ clusters, while **2** and **3** possess a parallel and a inclined 2D → 3D polycatenated framework, respectively.

Three unique MOFs constructed by 1,4-bis(4-pyridyl)-2,3-diaza-1,3-butadiene and dicarboxylates: from rhombic tetrameric Zinc(II) 2D layer to 2D + 2D → 3D polycatenated frameworks

Jie Zhou [a], Tong Yan [a], Yong-Feng Qiao [a], Yi-Dan Zhao [a], Xiao Wang [a], Lin Du [a], Ming-Jin Xie [a], Jian Xu [a], Qi-Hua Zhao [a]*

[a] *Key Laboratory of Medicinal Chemistry for Natural Resource Education Ministry, School of Chemical Science and Technology, Yunnan University, Kunming, 650091, P. R. China*

* Corresponding Author. Tel: +86 871 5032929; fax: +86 871 5032929. E-Mail: qhzhao@ynu.edu.cn

Highlights

(1) Complex **1** has a unique 2D double-layered framework containing rhombic tetrameric Zn(II) of mixed T_d and O_h geometries.
(2) Complex **2** shows a 2D + 2D → 3D parallel polycatenated framework which contains two-dimensional bilayers with cuboids as the fundamental building units.
(3) Complex **3** possess an interesting 2D → 3D inclined polycatenation net based on 4^4-**sql** subunits.
(4) The photoluminescent properties of **1** and **2**, and magnetic properties of **3** were studied.